JOC The Journal of Organic Chemistry

Article

pubs.acs.org/joc

Density Functional and Kinetic Monte Carlo Study of Cu-Catalyzed Cross-Dehydrogenative Coupling Reaction of Thiazoles with THF

Yuping Cai,[†,¶] Sheng'en Zhang,[†,¶] Yunsheng Xue,[†,‡] Juli Jiang,[§] and Zhao-Xu Chen*[,†]

[†]Key Laboratory of Mesoscopic Chemistry of MOE, Institute of Theoretical and Computational Chemistry, School of Chemistry and Chemical Engineering, Nanjing University, Nanjing 210093, P. R. China

[‡]School of Pharmacy, Xuzhou Medical College, No. 209, Tongshan Road, Xuzhou 221004, P. R. China

[§]Center for Multimolecular Chemistry, School of Chemistry and Chemical Engineering, Nanjing University, Nanjing 210093, P. R. China

Supporting Information

ABSTRACT: Cu-catalyzed cross-dehydrogenative coupling (CDC) reaction of thiazoles with THF has been studied with the density functional theory method and kinetic Monte Carlo (kMC) simulations. Our results show that the previously proposed concerted metalation−deprotonation mechanism is unfavorable. On the basis of the DFT calculation and kMC simulation results, a new mechanism is proposed. In the favorable mechanism, the Cu(II) catalyst first combines with the thiazoles, forming an organocopper species that then binds to the THF radical. The rate-limiting step, C−C bond formation, is realized through an intramolecular structural rearrangement. The Cu catalyst works as a matchmaker to render the C−C bond formation. Kinetic Monte Carlo simulations demonstrate that one should be careful with the conclusions drawn simply from the calculated barriers.

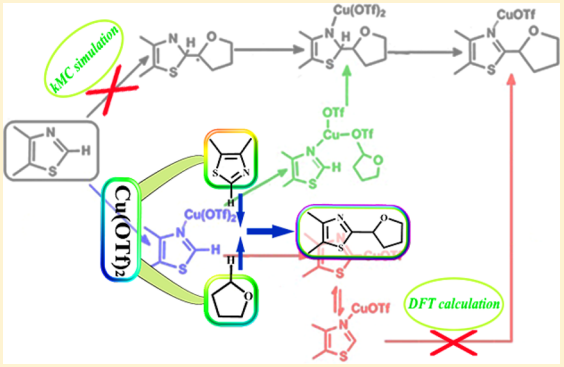

1. INTRODUCTION

Azoles, especially thiazoles and benzothiazoles, are widespread in various products,[1,2] from agricultural and pharmaceutical agents to material sciences.[3−5] The functionalization of C−H bonds in azoles can lead to valuable compounds,[6−9] from which inspiring progress on transition-metal-catalyzed reactions of azoles has been made.[10,11] For example, Zhang et al. developed a straightforward protocol for direct oxidative cross-coupling of electron-deficient perfluoroarenes with aromatic heterocycles using a Pd catalyst. Cross-coupling reactions of nucleophiles with electrophiles are powerful synthetic tools to create carbon−carbon (C−C) bonds.[12−17] Because of the shortness of synthetic routes and of atom-economics as well as unnecessary preparation of oriented and activated groups,[18,19] direct cross-dehydrogenative coupling (CDC) reactions are particularly useful in synthetic organic chemistry.[20−23] In fact, numerous examples of C−C, C−N, and C−P bond formation by CDC reactions in azoles are reported.[24−43] In CDC reactions, noble metals are widely used. Application of nonprecious metals, such as copper[43] and iron,[40] remains limited and is still a big challenge.

Recently, we reported a copper-catalyzed CDC reaction of thiazoles, shown in eq 1.[44] The reaction was carried out with a

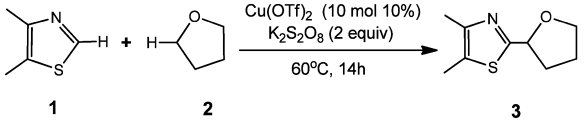

1 2 3 (1)

catalytic amount of copper(II) triflate ($Cu(OTf)_2$) in the presence of tetrahydrofuran (THF) at 60 °C under a N_2 atmosphere. Potassium peroxydisulfate acted as the oxidant. We found only a C2-thiazole product was produced, and various thiazoles ranging from electron-rich to -deficient could be used with yields up to 90%.

A few theoretical studies on some Cu-catalyzed C−H activation are available.[45−50] Wu et al. found that $Cu(OTf)_2$-catalyzed arylation of anilide proceeds via a Heck-like four-membered-ring transition state involving a Cu^{III}−Ph species, and the calculated barrier is approximately 25 kJ/mol for the most preferred pathway.[45] Lin et al. proposed a four-membered concerted metalation-deprotonation (CMD) transition state for the coupling of Ar−H with PhI.[46] Fu et al. suggested that a CMD mechanism is favored for Cu-catalyzed intramolecular C−H activation. Three steps are included in this mechanism: CMD with Cu(II), oxidation of the Cu(II) intermediate, and reductive elimination from Cu(III).[49] However, Santoro et al. performed density functional theory calculations to study the reaction mechanism and origins of C2 selectivity in a copper(I)-catalyzed amidation of indoles.[48] They demonstrated that the CMD mechanism cannot rationalize the observed regioselectivity and proposed a mechanism based on a four-center reductive elimination. Recently, Wu, Wiest, and Zhang studied theoretically the reaction mechanism of the Cu-catalyzed oxidative CDC

Received: October 30, 2015
Published: January 21, 2016

DOI: 10.1021/acs.joc.5b02503
J. Org. Chem. 2016, 81, 1806−1812

reaction involving sp^3-C−H bond activation.[50] Their results supported an SET mechanism but also uncovered an alternative mechanism in which O_2 is directly involved in a hydrogen-abstracting step.

Previously, we proposed a reaction mechanism, shown in Scheme 1, to rationalize the reaction process.[44] In this mechanism, $Cu(OTf)_2$ first reacts with the substrate thiazoles **1** to yield organocopper species **A**. Then, the reactive intermediate **B′** is generated from reaction of organocopper species **A** with the THF radical produced from the oxidation of $S_2O_8^{2-}$. Finally, the desired CDC reaction product **3** is produced by a reductive elimination of Cu(OTf) from species **B′**. However, no thorough theoretical investigation has been conducted to verify the above mechanism.

Scheme 1. Previously Proposed Mechanism for Cu-Catalyzed CDC Reaction

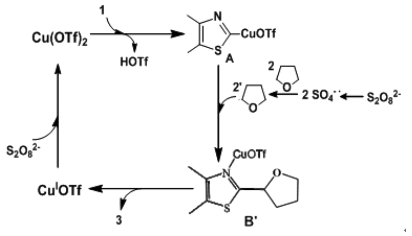

To obtain a deeper understanding of the mechanism of the C−C bond formation between THF and thiazoles through the CDC reaction, we carried out a detailed density functional investigation on the reaction potential energy surface of the Cu-catalyzed cross-dehydrogenative coupling reaction of 4,5-dimethylthiazole with THF. Our results do not support the mechanism proposed previously in ref 44. On the basis of the DFT calculations and kinetic Monte Carlo simulation results, a new mechanism is proposed. In the mechanism, thiazoles **1** first combine $Cu(OTf)_2$ through the coordination of the Cu atom to the N atom in **1**. Then, a THF radical produced by oxidation of $S_2O_8^{2-}$ binds to OTf of the complex, forming intermediate **5**. Intramolecular C−C bond formation in **5**, which is the rate-limiting step, takes place, leading to intermediate **6**. After stepwise losing HOTf and CuOTf from **6**, final product **3** is generated. The role of $Cu(OTf)_2$ works as a matchmaker. It anchors thiazoles and THF in a position favorable for the C−C bond formation.

2. RESULTS AND DISCUSSION

2.1. Three Reaction Routes to the Final Product. Scheme 2 shows our calculated catalytic cycle and reaction heats and barriers (in parentheses). Experimentally, it is found that final product **3** would not be produced without the oxidant $K_2S_2O_8$, likely owing to absence of THF radical intermediate **2′**. It is suggested[15] that **2′** is formed through the process illustrated at top left of Scheme 2. In this process, the $S_2O_8^{2-}$ anion first dissociates into two SO_4^{-}·.[51,52] Our calculations show that this step is endothermic by 116.8 kJ/mol. The formed SO_4^{-}· captures a hydrogen from THF, producing radical intermediate **2′**, releasing 41.6 kJ/mol. Below, we consider three possible reaction routes.

*Route I (**1** → **4** → **A** ↔ **A′** → **B′** → **3**).* This route starts from a combination of 4,5-dimethylthiazole (**1**) and tetradentate copper complex $Cu(OTf)_2$, forming organocopper species **4**. This step is a strongly exothermic process, releasing 117.8 kJ/mol. It is simply a coordination process of the $Cu(OTf)_2$ to the N atom of species **1** and is essentially a barrier-free process. In organocopper species **4**, the copper atom forms roughly a planar square with the four coordination atoms (N, O, O, and O) (Figure 1). The N−Cu bond is 1.97 Å, and the three Cu−O bonds are 2.06, 2.06, and 1.92 Å (Figure 1). Species **4** loses HOTf to form tetradentate copper complex **A**. The copper atom in **A** also forms

Scheme 2. Proposed Mechanism for Cu-Catalyzed CDC Reaction between 1 and THF[a]

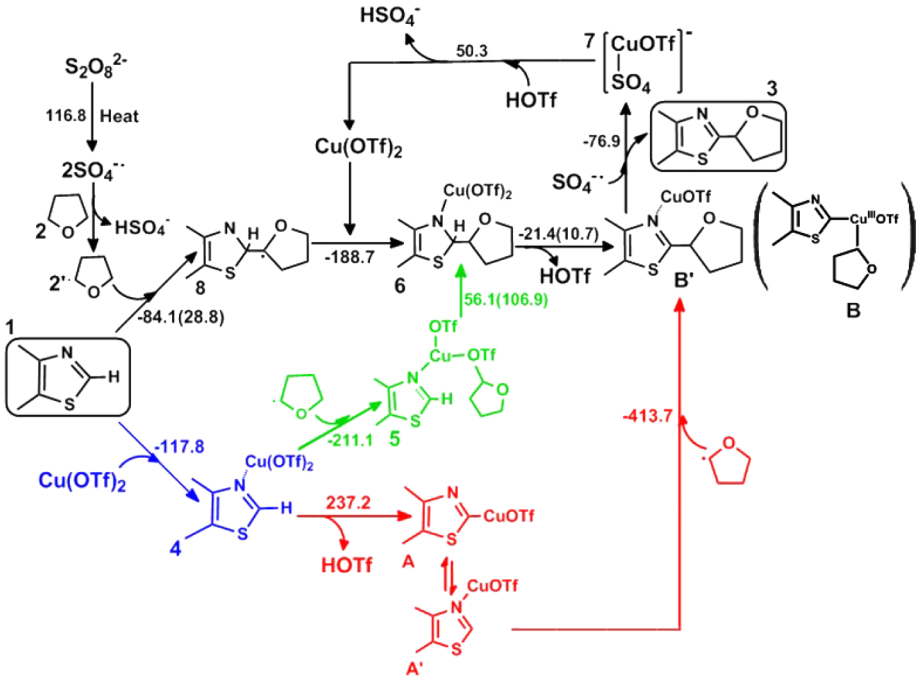

[a]Reaction heats and barriers (in parentheses) in kJ/mol.

DOI: 10.1021/acs.joc.5b02503
J. Org. Chem. 2016, 81, 1806−1812

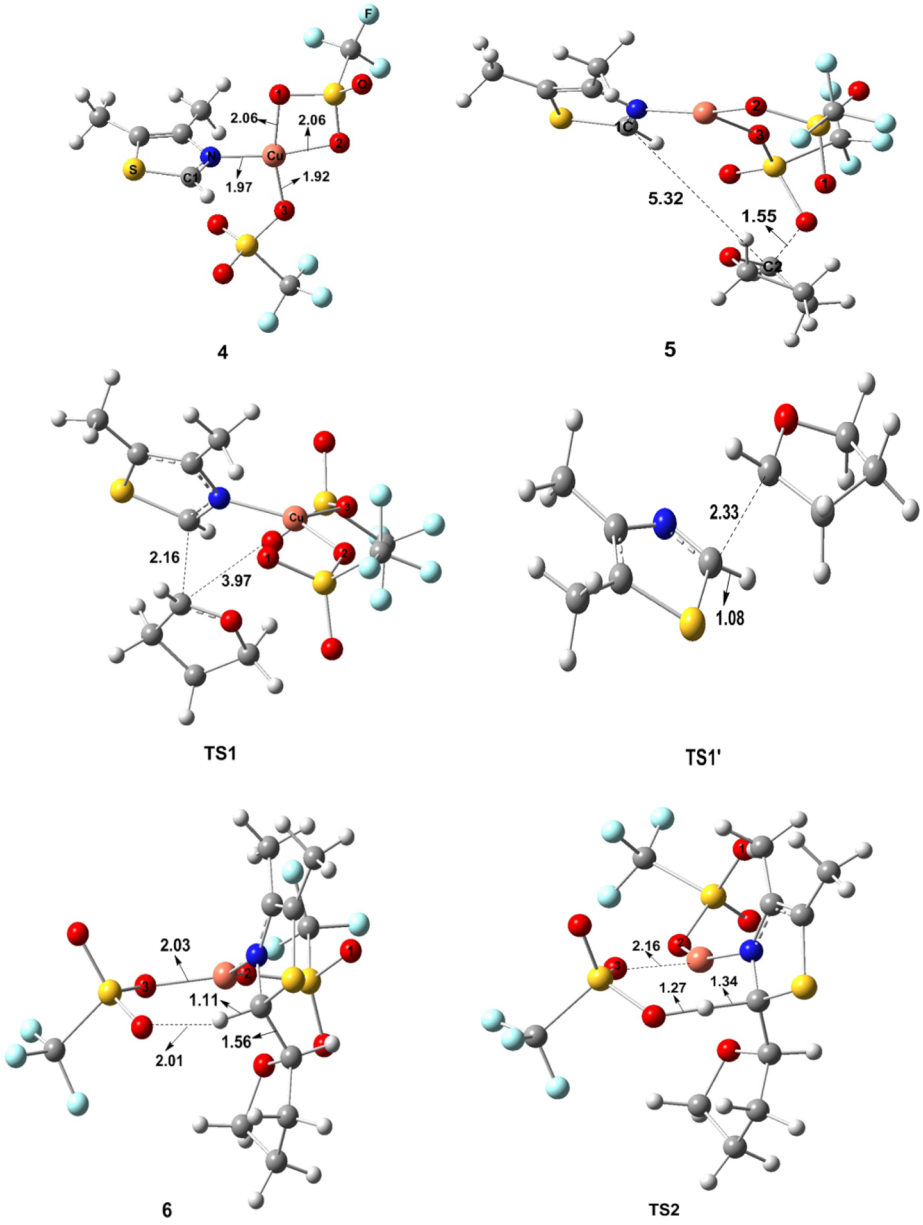

Figure 1. Structural illustration of some species with bond distances in Å.

basically a planar square with four coordination atoms (C, N, O, and O) (Figure S1) just as in **4**. Our calculations show that species **A** has a bidentate isomer **A′**. The stability difference between **A** and **A′** is less than 0.5 kJ/mol. A reaction heat of 237.2 kJ/mol is calculated from **4** to **A**, implying that this step is kinetically very unfavorable because the barrier must be ≥237.2 kJ/mol. The formed **A** isomerizes to **A′**; then, **A′** reacts with **2′** and generates **B′** (Figure S1). In **B′**, the C atom of **2′** binds to the C atom in **A′**. Previously,[44] we found that species **B′** has two energetically very unfavorable isomers: **B** and H-transferred **B** (Figure S1). In **B**, the Cu atom bonds to the C atom in thiazole and to the O atom in OTf with the Cu−C and Cu−O distances being 1.893 and 1.916 Å, respectively (Figure S1). The distance between the Cu and the radical C in **2′** is 2.380 Å. The H-transferred **B** is formed upon an easy transformation of one of the H atoms of species **2′** to the N atom (Figure S1). In H-transferred **B**, the Cu−C length is optimized to be 3.799 Å, showing that there is no strong interaction between them. Isomers **B** and H-transferred **B** are 250 and 143 kJ/mol less stable than species **B′**, respectively. Hence, thermodynamically, **B′** is much more favorable than **B** and H-transferred **B**. In fact, formation of **B′** is a strong exothermic process that releases 413.7 kJ/mol. In the final step of Route I, **B′** loses CuOTf and produces final product **3**, releasing 76.9 kJ/mol.

*Route II (**1** → **4** → **5** → **6** → **B′** → **3**).* The first step in Route II, formation of **4** from **1** and $Cu(OTf)_2$, is the same as in Route I. The difference between Route II and Route I starts from the reaction of **4**: Whereas **4** loses HOTf to become **A** in Route I, it combines **2′** to form **5** and release 211.1 kJ/mol in Route II. The formed **5** isomerizes to intermediate species **6**. Here, we can see that the Cu catalyst works as a matchmaker to render the formation of the C−C bond. The C−C formation experiences a transition state TS1 by circumventing a barrier of 106.9 kJ/mol and absorbing a heat of 56.0 kJ/mol. In the transition state TS1, the C−C bond shrinks from 5.32 Å in **5** to 2.16 Å (Figure 1). In species **6**, the C−C bond between thiazoles and THF becomes

DOI: 10.1021/acs.joc.5b02503
J. Org. Chem. 2016, 81, 1806−1812

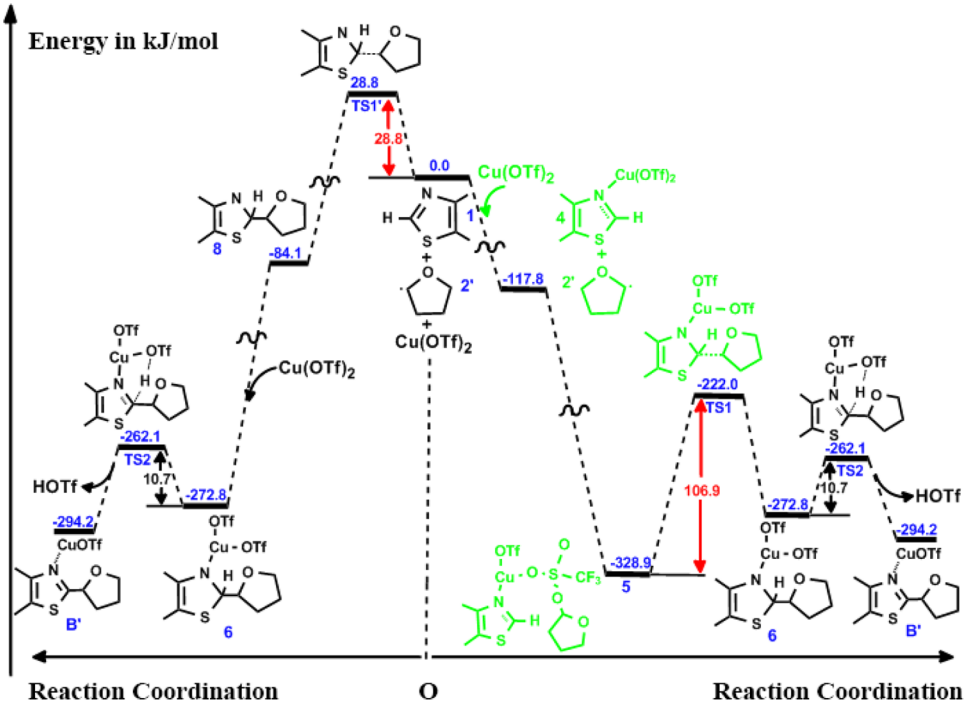

Figure 2. Two possible pathways for Cu-Catalyzed C−C formation.

1.56 Å, which shows that it has been formed. Complex **6** undergoes reductive elimination of HOTf to afford species **B′** via a transition state (TS2, Figure 1). The C−H bond, 1.11 Å in complex **6**, becomes 1.34 Å in TS2. Obviously, the C−H bond has been weakened greatly. The energy barrier of this step is only 10.7 kJ/mol. With the help of $SO_4^{-\bullet}$, **B′** loses CuOTf and becomes product **3**.

*Route III (**1** → **8** → **6** → **B′** → **3**).* In this route, thiazole **1** first combines with the formed radical **2′** directly, forming **8**. This process experiences a transition state TS1′ (Figure 1), circumventing a barrier of 28.8 kJ/mol with a heat of −84.1 kJ/mol. The C−C bond is 2.33 Å in TS1′, and it becomes 1.54 Å in complex **8**. The formed **8** reacts with $Cu(OTf)_2$, forming complex **6** and releasing heat of −188.7 kJ/mol. This step is essentially a barrier-free process. Then, **6** loses HOTf to generate **B′**, and finally **B′** loses CuOTf to yield product **3** as in Routes I and II.

Previously, we[44] had theoretically examined the reaction pathway starting from **A** (**A** ↔ **A′** → **B′** → **3**). In that study, it is implicitly assumed that **A** can be easily formed.[53,54] As shown in Scheme 2, the barrier from **4** to **A** is ≥237.2 kJ/mol. Obviously, Route I cannot compete with Route II, which has a barrier of 106.9 kJ/mol for the rate-limiting step **5** → **6**. In fact, **4** → **5** in Route II is a barrier-free and strongly exothermic (by −211.1 kJ/mol) process. Thus, it is safe to conclude that **4** will react with **2′** to produce **5** preferentially, and **A** or **A′** can hardly be formed. Hence, our present calculations clearly show that Route I is least likely and can be excluded as the main route for the formation of **3**.

Comparing Routes II and III, one can see that the barrier of the rate-limiting step of Route II, 106.9 kJ/mol for **5** → **6**, is much higher than that of Route III, 28.8 kJ/mol for **1** → **8**. On the basis of rate-limiting step barriers, one would expect that Route III would dominate the formation of **3**. We will present a kinetic Monte Carlo simulation to answer this question in the next section. Figure 2 summarizes the calculated potential energy surfaces for the formation of **B′**.

As soon as **B′** is formed, $SO_4^{-\bullet}$ will act on it, producing final product **3** along with species **7**. This process will release 76.9 kJ/mol. In terms of thermodynamics, it is a favorable process. Without $SO_4^{-\bullet}$ direct pyrolysis of **B′** to yield **3** needs to absorb 198.4 kJ/mol. This result manifests the role played by $SO_4^{-\bullet}$ in the reaction cycle. $Cu(OTf)_2$ is produced by the reaction of **7** with HOTf produced from **6** to **B′**. This step is endothermic by 50.3 kJ/mol. The produced $Cu(OTf)_2$ then reenters the cycle by reacting with **1** or **8**.

2.2. Kinetic Monte Carlo Simulations. As mentioned above, we have located two pathways that can lead to **3**, starting from the three reactants. Figure 2 shows the potential energy surface from the reactants to **B′**, and we did not extend to **3** because Routes II and III go through the same route from **B′** to **3**. Note the barrier of the rate-determining step is only 28.8 kJ/mol for the left pathway (Route III) whereas that of the right pathway (Route II) is 106.9 kJ/mol. At first glance, **B′** produced from the left will be dominant. However, **1** can be transformed to **5** via a barrier-free process, which will deplete the reactants very fast and thus reduce the contribution to **B′** formation from the left pathway. At this stage, one question arises: which pathway dominates the production of **B′**? To answer this question, we used the kinetic Monte Carlo method[55] to simulate the reaction network presented in Figure 2, using the DFT calculated pre-exponential factors and rate constants for each reaction presented in the Supporting Information.

Figure 3 shows the time evolution of the final product **B′** produced through the right pathway and denoted as **B′R**. **B′** produced via the left pathway is close to 0 and is not shown in Figure 3. The simulation result clearly shows that **B′** is almost exclusively produced from the right pathway. Note that the barrier heights of the rate-limiting step are 28.8 and 106.9 kJ/mol for the left and right pathways, respectively. The present simulations indicate that one cannot judge the contribution of a

DOI: 10.1021/acs.joc.5b02503
J. Org. Chem. 2016, 81, 1806−1812

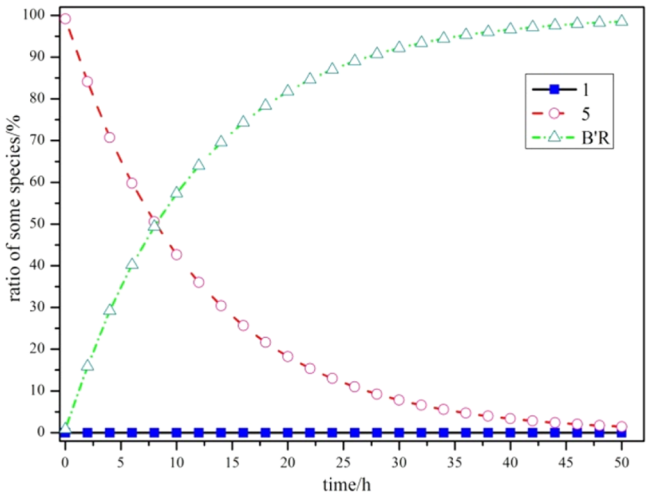

Figure 3. Time evolution of **1**, **5**, and **B′** produced from the right pathway in Figure 2.

pathway simply by considering the energy barrier height of the rate-limiting step. From Figure 3, one can see that the concentration of **1** decreases to ∼0 whereas that of **5** shoots up to ∼100% in a very short time, indicating that nearly all of the reactants are instantly converted to **5**. This is obviously because the formation of **5** from **1** via stepwise complexation with $Cu(OTf)_2$ and then with THF is a barrier-free process. This complexation reaction overwhelms the reaction from **1** to **8** even though the latter has a quite low barrier of only 28.8 kJ/mol. With increasing time, formed **5** gradually transforms into **B′**. According to our simulation (Figure 3), **B′** reaches 86% after 24 h compared to 14 h experimentally.

From the PES shown in Figure 2, one may expect that the equilibrium concentration of **5** should be higher than that of **B′**, which is inconsistent with our simulation (Figure 3 indicates that the percentage of **B′** reaches 99%, whereas that of **5** is less than 1% after 50 h). Analysis reveals that this is because the rate constant of reaction **6** → **B′** (4.18×10^9) is extremely large compared with those of **B′** → **6** (8.21×10^{-4}) and **6** → **5** (4.86×10^4) (Table S1). To examine the influence of the rate constants (of course, essentially this is because the PES is not Gibbs free energy based) on the equilibrium concentration of **5** and **B′**, we set the forward and backward reaction rate constants of **6** → **B′** to be 4.18×10^4 and 8.21×10^4, respectively, while keeping the other constants unchanged. In this case, we have $k_{5\to6} \ll k_{6\to5} \approx k_{6\to B'} \approx 1/2k_{B'\to6}$. We found that the percentage of **5** reaches 100% very quickly whereas the ones of both **6** and **B′** are next to 0 (Figure 4). If we keep $k_{6\to5}$ unchanged and set $k_{5\to6}$, $k_{6\to B'}$, and $k_{B'\to6}$ to be 2.27×10^4, 4.18×10^4, and 8.21×10^4, respectively (in this case, $k_1 \approx k_2 \approx k_3 \approx 1/2k_4$), the equilibrium percentages of **5**, **6**, and **B′** become 58, 27, and 14%, respectively, consistent with our expectation.

3. CONCLUSIONS

We have studied the mechanism of Cu-catalyzed cross-dehydrogenative coupling reaction of thiazoles with THF. We show that this reaction does not follow the previously assumed Cu(II)-assisted concerted metalation−deprotonation (CMD) mechanism. In the favorable mechanism, the Cu(II) catalyst first combines with the thiazoles, forming an organocopper species **4**. Then, species **4** binds to a THF radical via the C−O interaction, forming **5**. The C−C bond formation is realized through an intramolecular structural rearrangement. The Cu catalyst works as a matchmaker to render the occurrence of C−C bond formation. The rate-limiting step is formation of the C−C bond. Another route, in which the Cu(II) catalyst attacks intermediate **8** formed by the combination of thiazoles with THF, may compete with the favorable route. Kinetic Monte Carlo simulations demonstrate that the latter route hardly contributes to the production of the final product because the formation of **5** is a barrier-free process, which makes the formation of **8** impossible. This result also indicates that one should be careful when drawing conclusions simply based on the barriers. Finally, we reveal that the role of potassium peroxydisulfate is to produce sulfate radical anion without which transformation of **B′** to final product **3** is difficult, which is in agreement with the experimental observation.

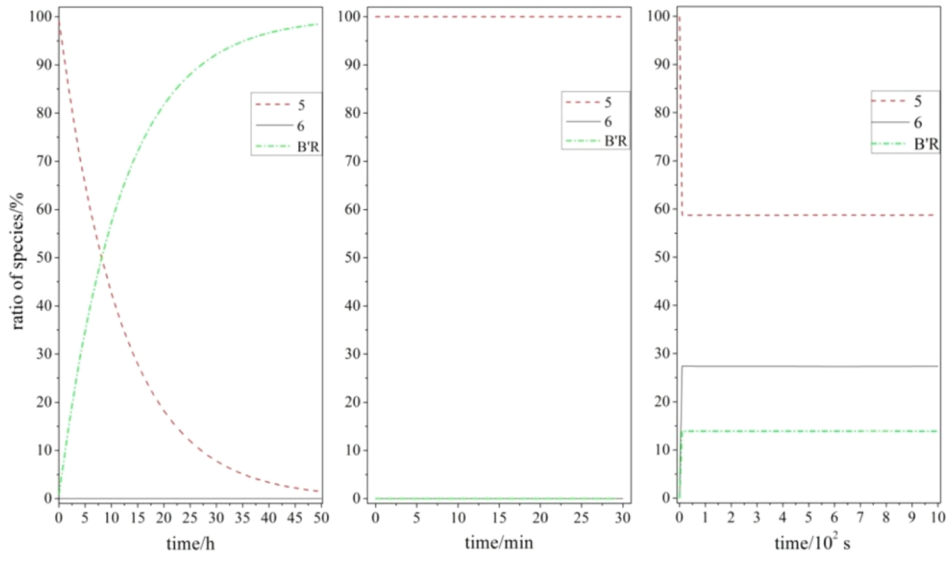

Figure 4. Time evolution of **5**, **6**, and **B′R**.

DOI: 10.1021/acs.joc.5b02503
J. Org. Chem. 2016, 81, 1806−1812

4. EXPERIMENTAL SECTION

Computational Methods. All of the calculations were performed with the Gaussian09 package.[56] Geometry optimization of all the minima and transition states involved was carried out at the B3LYP[57,58] level with the Lanl2DZ[59] basis set for Cu and 6-31G(d) for C, H, O, N, and S. Default convergence criteria were used. The vibrational frequency calculations were conducted at the same level of theory as geometry optimization to confirm whether each optimized structure is an energy minimum or a saddle point. For each transition state, intrinsic reaction coordinate (IRC) analysis[60] was performed to verify that it connects the right reactants and products on the potential energy surface. The solvent effects were considered using the PCM model[61,62] with the gas-phase-optimized structures as the initial geometries.

■ ASSOCIATED CONTENT

Supporting Information

The Supporting Information is available free of charge on the ACS Publications website at DOI: 10.1021/acs.joc.5b02503.

Optimized structures of some key stationary points in PES, pre-exponential factors and rate constants used in kMC simulations, and energetics and Cartesian coordinates of key stationary points (PDF)

■ AUTHOR INFORMATION

Corresponding Author

*E-mail: zxchen@nju.edu.cn.

Author Contributions

¶Y.-P.C. and S.-E.Z. contributed equally.

Notes

The authors declare no competing financial interest.

■ ACKNOWLEDGMENTS

We gratefully thank the financial support from the National Basic Research Program of China (973 program, 2011CB808604) and the National Natural Science Foundation of China (NSFC, No. 21273103).

■ REFERENCES

(1) DeSimone, R. W.; Currie, K. S.; Mitchell, S. A.; Darrow, J. W.; Pippin, D. A. *Comb. Chem. High Throughput Screening* **2004**, *7*, 473.
(2) Hili, R.; Yudin, A. K. *Nat. Chem. Biol.* **2006**, *2*, 284.
(3) Lewis, J. C.; Bergman, R. G.; Ellman, J. A. *Acc. Chem. Res.* **2008**, *41*, 1013.
(4) Corbet, J. P.; Mignani, G. *Chem. Rev.* **2006**, *106*, 2651.
(5) Ricci, A. *Amino Group Chemistry, From Synthesis to the Life Sciences*; Wiley-VCH: Weinheim, 2007.
(6) Marion, N.; Nolan, S. P. *Acc. Chem. Res.* **2008**, *41*, 1440.
(7) Armstrong, A.; Collins, J. C. *Angew. Chem., Int. Ed.* **2010**, *49*, 2282.
(8) Enders, D.; Niemeier, O.; Henseler, A. *Chem. Rev.* **2007**, *107*, 5606.
(9) Nair, V.; Vellalath, S.; Babu, B. P. *Chem. Soc. Rev.* **2008**, *37*, 2691.
(10) Schnurch, M.; Flasik, R.; Khan, A. F.; Spina, M.; Mihovilovic, M. D.; Stanetty, P. *Eur. J. Org. Chem.* **2006**, *2006*, 3283.
(11) He, C. Y.; Fan, S. L.; Zhang, X. G. *J. Am. Chem. Soc.* **2010**, *132*, 12850.
(12) Zhao, D. B.; You, J. S.; Hu, C. W. *Chem. - Eur. J.* **2011**, *17*, 5466.
(13) Ackermann, L. *Chem. Rev.* **2011**, *111*, 1315.
(14) Wencel-Delord, J.; Droge, T.; Liu, F.; Glorius, F. *Chem. Soc. Rev.* **2011**, *40*, 4740.
(15) Chiusoli, G. P.; Catellani, M.; Costa, M.; Motti, E.; Della Ca', N.; Maestri, G. *Coord. Chem. Rev.* **2010**, *254*, 456.
(16) Colby, D. A.; Bergman, R. G.; Ellman, J. A. *Chem. Rev.* **2010**, *110*, 624.
(17) McGlacken, G. P.; Bateman, L. M. *Chem. Soc. Rev.* **2009**, *38*, 2447.
(18) Li, C. J. *Acc. Chem. Res.* **2009**, *42*, 335.
(19) Scheuermann, C. J. *Chem. - Asian J.* **2010**, *5*, 436.
(20) Le Bras, J.; Muzart, J. *Chem. Rev.* **2011**, *111*, 1170.
(21) Yeung, C. S.; Dong, V. M. *Chem. Rev.* **2011**, *111*, 1215.
(22) Girard, S. A.; Knauber, T.; Li, C. J. *Angew. Chem., Int. Ed.* **2014**, *53*, 74.
(23) Guin, S.; Rout, S. K.; Banerjee, A.; Nandi, S.; Patel, B. K. *Org. Lett.* **2012**, *14*, 5294.
(24) Wu, G.; Zhou, J.; Zhang, M.; Hu, P.; Su, W. P. *Chem. Commun.* **2012**, *48*, 8964.
(25) Kitahara, M.; Umeda, N.; Hirano, K.; Satoh, T.; Miura, M. *J. Am. Chem. Soc.* **2011**, *133*, 2160.
(26) Xi, P. H.; Yang, F.; Qin, S.; Zhao, D. B.; Lan, J. B.; Gao, G.; Hu, C. W.; You, J. S. *J. Am. Chem. Soc.* **2010**, *132*, 1822.
(27) Banerjee, A.; Santra, S. K.; Guin, S.; Rout, S. K.; Patel, B. K. *Eur. J. Org. Chem.* **2013**, *2013*, 1367.
(28) Dong, J. X.; Huang, Y. M.; Qin, X. R.; Cheng, Y. Y.; Hao, J.; Wan, D. Y.; Li, W.; Liu, X. Y.; You, J. S. *Chem. - Eur. J.* **2012**, *18*, 6158.
(29) Han, W.; Mayer, P.; Ofial, A. R. *Angew. Chem., Int. Ed.* **2011**, *50*, 2178.
(30) Do, H. Q.; Daugulis, O. *J. Am. Chem. Soc.* **2009**, *131*, 17052.
(31) Xia, Q. Q.; Chen, W. Z. *J. Org. Chem.* **2012**, *77*, 9366.
(32) Sang, P.; Xie, Y. J.; Zou, J. W.; Zhang, Y. H. *Org. Lett.* **2012**, *14*, 3894.
(33) Wang, Q.; Schreiber, S. L. *Org. Lett.* **2009**, *11*, 5178.
(34) Li, Y. M.; Xie, Y. S.; Zhang, R.; Jin, K.; Wang, X. N.; Duan, C. Y. *J. Org. Chem.* **2011**, *76*, 5444.
(35) Wang, J. A.; Hou, J. T.; Wen, J.; Zhang, J.; Yu, X. Q. *Chem. Commun.* **2011**, *47*, 3652.
(36) Kim, J. Y.; Cho, S. H.; Joseph, J.; Chang, S. *Angew. Chem., Int. Ed.* **2010**, *49*, 9899.
(37) Hou, C. D.; Ren, Y. L.; Lang, R.; Hu, X. X.; Xia, C. G.; Li, F. W. *Chem. Commun.* **2012**, *48*, 5181.
(38) Xiang, C. B.; Bian, Y. J.; Mao, X. R.; Huang, Z. Z. *J. Org. Chem.* **2012**, *77*, 7706.
(39) Mu, X. J.; Zou, J. P.; Qian, Q. F.; Zhang, W. *Org. Lett.* **2006**, *8*, 5291.
(40) Correa, A.; Fiser, B.; Gomez-Bengoa, E. *Chem. Commun.* **2015**, *51*, 13365.
(41) Chen, X. P.; Cui, X. L.; Yang, F. F.; Wu, Y. J. *Org. Lett.* **2015**, *17*, 1445.
(42) Aruri, H.; Singh, U.; Sharma, S.; Gudup, S.; Bhogal, M.; Kumar, S.; Singh, D.; Gupta, V. K.; Kant, R.; Vishwakarma, R. A.; Singh, P. P. *J. Org. Chem.* **2015**, *80*, 1929.
(43) Fan, S. L.; Chen, Z.; Zhang, X. G. *Org. Lett.* **2012**, *14*, 4950.
(44) Xie, Z. Y.; Cai, Y. P.; Hu, H. W.; Lin, C.; Jiang, J. L.; Chen, Z. X.; Wang, L. Y.; Pan, Y. *Org. Lett.* **2013**, *15*, 4600.
(45) Chen, B.; Hou, X. L.; Li, Y. X.; Wu, Y. D. *J. Am. Chem. Soc.* **2011**, *133*, 7668.
(46) Xue, L. Q.; Lin, Z. Y. *Chem. Soc. Rev.* **2010**, *39*, 1692.
(47) Wang, M. Y.; Fan, T.; Lin, Z. Y. *Organometallics* **2012**, *31*, 560.
(48) Santoro, S.; Liao, R. Z.; Himo, F. *J. Org. Chem.* **2011**, *76*, 9246.
(49) Tang, S. Y.; Gong, T. J.; Fu, Y. *Sci. China: Chem.* **2013**, *56*, 619.
(50) Cheng, G. J.; Song, L. J.; Yang, Y. F.; Zhang, X. H.; Wiest, O.; Wu, Y. D. *ChemPlusChem* **2013**, *78*, 943.
(51) Ledwith, A.; Russell, P. J.; Sutcliffe, Lh *J. Chem. Soc. D* **1971**, 964.
(52) Liu, Y. K.; Jiang, B.; Zhang, W.; Xu, Z. Y. *J. Org. Chem.* **2013**, *78*, 966.
(53) Gorelsky, S. I.; Lapointe, D.; Fagnou, K. *J. Am. Chem. Soc.* **2008**, *130*, 10848.
(54) Garcia-Cuadrado, D.; de Mendoza, P.; Braga, A. A. C.; Maseras, F.; Echavarren, A. M. *J. Am. Chem. Soc.* **2007**, *129*, 6880.
(55) Gillespie, D. T. *J. Comput. Phys.* **1976**, *22*, 403.
(56) Frisch, M. J. T, G. W.; Schlegel, H. B.; Scuseria, G. E.; Robb, M. A.; Cheeseman, J. R.; Scalmani, G.; Barone, V.; Mennucci, B.; Petersson, G. A.; Nakatsuji, H.; Caricato, M.; Li, X.; Hratchian, H. P.; Izmaylov, A. F.; Bloino, J.; Zheng, G.; Sonnenberg, J. L.; Hada, M.; Ehara, M.; Toyota, K.; Fukuda, R.; Hasegawa, J.; Ishida, M.; Nakajima, T.; Honda, Y.; Kitao, O.; Nakai, H.; Vreven, T.; Montgomery, J. A., Jr.; Peralta, J. E.; Ogliaro, F.; Bearpark, M.; Heyd, J. J.; Brothers, E.; Kudin, K. N.; Staroverov, V. N.; Keith, T.; Kobayashi, R.; Normand, J.; Raghavachari, K.; Rendell, A.;

DOI: 10.1021/acs.joc.5b02503
J. Org. Chem. 2016, 81, 1806−1812

Burant, J. C.; Iyengar, S. S.; Tomasi, J.; Cossi, M.; Rega, N.; Millam, J. M.; Klene, M.; Knox, J. E.; Cross, J. B.; Bakken, V.; Adamo, C.; Jaramillo, J.; Gomperts, R.; Stratmann, R. E.; Yazyev, O.; Austin, A. J.; Cammi, R.; Pomelli, C.; Ochterski, J. W.; Martin, R. L.; Morokuma, K.; Zakrzewski, V. G.; Voth, G. A.; Salvador, P.; Dannenberg, J. J.; Dapprich, S.; Daniels, A. D.; Farkas, O.; Foresman, J. B.; Ortiz, J. V.; Cioslowski, J.; Fox, D. J. *Gaussian 09*, revision D.01; Gaussian, Inc.: Wallingford, CT, 2013.

(57) Becke, A. D. *J. Chem. Phys.* **1993**, *98*, 5648.

(58) Lee, C. T.; Yang, W. T.; Parr, R. G. *Phys. Rev. B: Condens. Matter Mater. Phys.* **1988**, *37*, 785.

(59) Hay, P. J.; Wadt, W. R. *J. Chem. Phys.* **1985**, *82*, 270.

(60) Gonzalez, C.; Schlegel, H. B. *J. Phys. Chem.* **1990**, *94*, 5523.

(61) Barone, V.; Cossi, M.; Tomasi, J. *J. Chem. Phys.* **1997**, *107*, 3210.

(62) Tomasi, J.; Mennucci, B.; Cammi, R. *Chem. Rev.* **2005**, *105*, 2999.

DOI: 10.1021/acs.joc.5b02503
J. Org. Chem. 2016, 81, 1806−1812